ELSEVIER

Superlattices and Microstructures 35 (2004) 657–668

Superlattices and Microstructures

www.elsevier.com/locate/superlattices

Quantification of the water boiling heat transfer in micro-structures by image analysis

C. Ferret[a,*], L. Falk[a], A. Chenu[a], U. D'Ortona[b], T.T. Veenstra[c]

[a] *CNRS-LSGC-ENSIC, 1 rue Grandville, 54000 Nancy, France*
[b] *CNRS-LMSNM, 38 rue Frederic Joliot Curie, 13451 Marseille Cedex 20, France*
[c] MESA$^+$ *Research Institute, University of Twente, PO Box 217, 7500 AE Enschede, The Netherlands*

Received 10 June 2003; received in revised form 10 October 2003; accepted 25 November 2003

Available online 22 July 2004

Abstract

The heat transfer performance of a micro-vaporizer has been measured by conventional methods (using temperatures, flow rates, effective power input). The study was carried out for laminar flow in channels (5 mm × 3 cm × 200 μm) micro-structured with square obstacles to increase the specific area. The results show that high heat transfer coefficients (1300–2500 W m^{-2}/°C^{-1}) can be reached in such a micro-structured channel. Image analysis was done to estimate the volume vapour fraction, which can be converted into the mass vapour fraction using a slip ratio and avoids the need for any temperature or electric power input measurements. The estimation of this slip ratio is discussed in this paper.

Keywords: Heat transfer; Micro-structure; Laminar; Boiling; Image analysis

1. Introduction

This study concerns the performance of a micro-vaporizer implemented in a micro-plant for hydrogen production [1] to supply a portable low power fuel cell (100 W). As the reactants (mixture of water and methanol) are fed in the liquid phase while the reactions in the reformer reactor take place in the gas phase, the first component of the micro-plant has to be a vaporizer. The required liquid flow rate to be vaporized is about 2 ml min^{-1} and the required exit temperature of the vapour is 260 °C.

* Corresponding author. Tel.: +33-3-83-17-51-04; fax: +33-3-83-17-50-94.
E-mail address: ferret@ensic.inpl-nancy.fr (C. Ferret).

0749-6036/$ - see front matter © 2004 Elsevier Ltd. All rights reserved.
doi:10.1016/j.spmi.2003.11.009

Nomenclature

Bo	Bond number (–)
Boi	Boiling number (–)
C_p	Specific heat (J kg^{-1} °C^{-1})
D_h	Hydraulic diameter (m)
g	Gravity acceleration (m s^{-2})
h	Heat transfer coefficient (W m^{-2} °C^{-1})
k	Thermal conductivity (W m^{-1} °C^{-1})
Nu	Nusselt number (–)
Nu_3	Laminar Nusselt number for three-wall heat transfer (–)
Nu_4	Laminar Nusselt number for four-wall heat transfer (–)
Q_h	Single-phase heat flux (W)
Q_m	Mass flow rate (kg s^{-1})
Q_tl	Thermal losses heat flux (W)
Q_tot	Total electric heat flux supplied (W)
Q_vap	Vaporization heat flux (W)
Re	Reynolds number (–)
S	Slip ratio (–)
T	Temperature (°C)
We	Weber number (–)
X	Mass vapour fraction (–)
y	Ratio of vapour to liquid volume flow rate (–)
Symbols	
α	Volume vapour fraction (–)
β	Aspect ratio of the channel (–)
ΔH_vap	Heat of vaporization (J kg^{-1})
ρ	Mass volume (kg m^{-3})
σ	Surface tension (N m^{-1})
τ	Time constant (s)
Ω	Heating surface (m^2)
Subscripts	
in	Inlet
out	Outlet
sat	Saturation
w	Wall
liq	Liquid
vap	Vapour

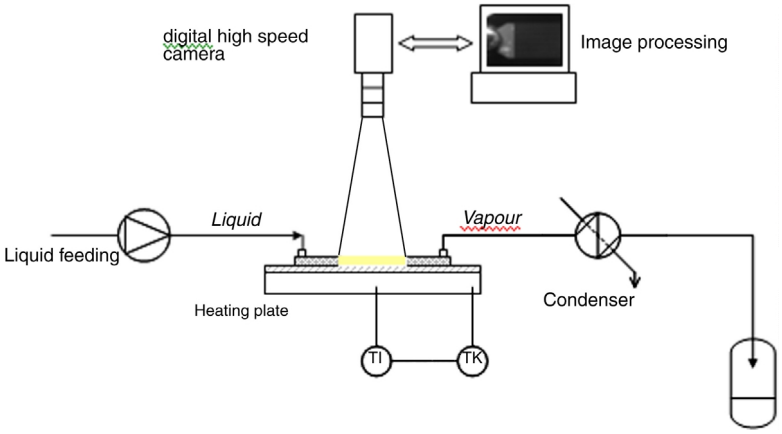

Fig. 1. The scheme of the experimental set-up.

In this paper preliminary results concerning the heat transfer coefficient measurements in such a micro-vaporizer are reported for pure water for several wall temperatures and flow rates.

The heat transfer has been estimated by two different methods: one based on classical heat transfer measurements such as wall temperatures, and a second based on the estimation of the vapour fraction. For this second method, the volume vapour fraction was measured at the outlet of the exchanger using a high speed camera coupled with an image analysis program. According to the heat balance equation, the estimation of the boiling heat transfer coefficient is based on the experimental value of the mass vapour fraction instead of the volume fraction which requires the knowledge of the slip ratio of the vapour velocity to the liquid velocity. The estimate of the slip ratio, S, was determined with the correlations of Hewitt [2], determined for conventional ducts. The experimental slip ratios, determined thanks to the first method, are compared with the correlation values to verify the validity of such a relation for micro-systems.

2. Experimental set-up

2.1. Testing bench description

The experimental set-up (Fig. 1) is composed of a HPLC pump to ensure a constant flow rate even for high pressure drop, the micro-structured plate heated by an electric resistance heater of 100 W, and a condenser for the vapour. The micro-structured plate is stuck on the electric heater with thermal grease which contains copper particles to ensure a high heat transfer. The temperature of the plate is homogeneous and controlled by a PID regulator.

The gas/liquid mixture at the outlet of the vaporizer is filmed using an enlarging high speed camera and the recorded images are used to estimate the vapour volume fraction.

The temperature profile of the wall along the micro-structured channel is measured using thermocouples (K type). The electric power input required to maintain the imposed temperature of the micro-channelled plate is measured as well with a precision of 0.1 W.

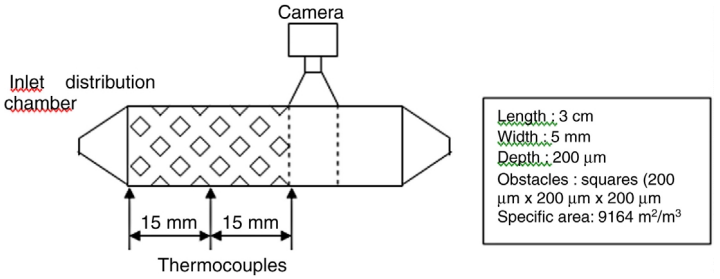

Fig. 2. The scheme of the micro-structured channel with location of the thermocouples for the wall temperature measurement.

The CCD camera has been used with a constant speed of 400 fps for all the experiments. A total duration of record of 5 s was a good compromise to optimize the time of treatment with a good accuracy for the estimation of the vapour volume.

2.2. The tested micro-structure

Preliminary experiments showed a strong fouling tendency of the system, even with the use of ultrapure water. Therefore a micro-filter (0.22 μm) was introduced between the pump and the plate to prevent the fouling of the system. The micro-channelled plate is made by assembling two different wafers (500 μm thickness each): one of silicon in which the channels are etched, and one made of Pyrex to cover the first one [3]. The liquid feeding is realized through holes drilled in the Pyrex on which bridles are glued.

Due to the vaporization of the liquid, bursts of vapour bubbles may flush the liquid through the channel and may reduce the liquid–wall contact area and moreover reduce the residence time of the liquid in the channel. Therefore the geometry used is an organized porous medium, which has been chosen both to increase the specific area and to prevent the entrainment of liquid droplets by the use of square obstacles (Fig. 2).

These plates were made by the Mesa$^+$ Research Institute at the University of Twente (Enschede, Netherlands).

3. Experimental procedure

3.1. Heat transfer measurements

During the experiments, both the wall temperature and the liquid flow rate at the inlet were imposed, whereas the inlet and outlet liquid temperatures and those along the channel have been measured.

Stationary conditions have been reached after several hours, which correspond to at least 5 times the time constant τ of the thermal equilibrium of the whole system. The time constant of the system is determined from the cooling curve.

The time constant τ of the system was measured by heating the plate with an imposed electric power until the temperature of the whole system became constant. Then the electric resistance heater was shut down and the temperature profile of the system was recorded over time (Fig. 3).

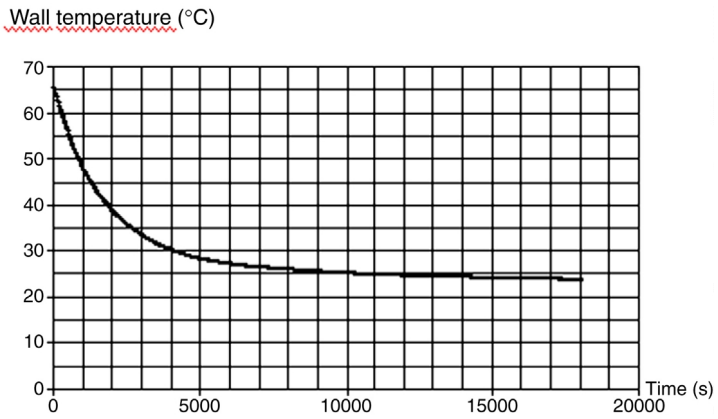

Fig. 3. The time–temperature profile of the wall for the determination of the system time constant.

The temperature profile can be fitted by a decay exponential law, corresponding to a first-order dynamic system, with a really good accuracy ($r^2 = 99.5\%$):

$$T = 24.3 + 39.5 * \exp(-0.000\,467 * t) \tag{1}$$

where 24.3 °C is the room temperature and 0.000 467 is the inverse of the time constant in seconds.

The time constant τ of the system is about 36 min, meaning that 63% of the steady state is reached at this time. To obtain 99% of the steady state, the waiting time is 5τ, which corresponds to about 3 h. For all the experiments it had been decided to wait for 3 h 30 min to reach stationary conditions.

3.2. Determination of the effective heat flux

The electric heat flux (Q_{tot}) supplied to the system to maintain the temperature at a constant value can be divided into three terms: the thermal losses (Q_{tl}), the effective heat flux to heat the liquid up to its saturation temperature (Q_{h}), and the one for performing the vaporization (Q_{vap}):

$$Q_{\text{tot}} = Q_{\text{tl}} + Q_{\text{h}} + Q_{\text{vap}}. \tag{2}$$

To estimate the thermal losses, the system was heated up to a given temperature without liquid circulation. When the stationary conditions are reached, the power input required to maintain the system at constant temperature is measured. This electric power corresponds to the thermal losses. Fig. 4 illustrates the evolution of the temperature of the system as a function of the electric power input (i.e. thermal losses), for two different room temperatures.

The heat flux (Q_{h}) needed to heat the liquid up to its boiling temperature can be calculated using the heat balance equation:

$$Q_{\text{h}} = Q_m \cdot C_p \cdot (T_{\text{inlet}} - T_{\text{sat}}). \tag{3}$$

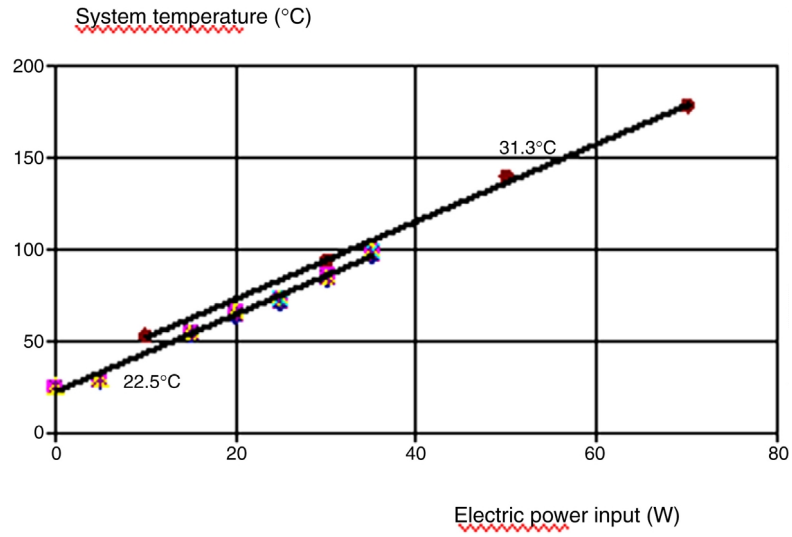

Fig. 4. Calibration of the system thermal losses to the environment for two room temperatures.

The estimation of the characteristic length scale of heating showed that the liquid reaches its boiling temperature within a few millimetres in the inlet distribution chamber. The liquid then enters in the micro-structured channel at its saturation temperature, so the micro-structured channel is completely devoted to the vaporization of the liquid. This assumption has been checked by CFD calculations.

The heat flux for vaporization can then be estimated by the difference between the electric power supplied to the system and the thermal losses and the heating fluxes:

$$Q_{\text{vap}} = Q_{\text{tot}} - (Q_{\text{tl}} + Q_{\text{h}}). \tag{4}$$

The boiling heat transfer coefficient, h, is then calculated from the heat balance:

$$h = \frac{Q_{\text{vap}}}{\Omega \cdot (T_{\text{w}} - T_{\text{sat}})}. \tag{5}$$

From the vaporisation flux and the mass flow rate it is also possible to determine the mass vapour fraction at the outlet:

$$X = \frac{Q_{\text{vap}}}{Q_m \cdot \Delta H_{\text{vap}}}. \tag{6}$$

3.3. Heat balance closing

In order to check the validity of the method, we have worked at a lower wall temperature (<100 °C) for which there is no boiling flow. In that case $Q_{\text{vap}} = 0$, and the combination of Eqs. (3) and (4) gives

$$Q_{\text{h}} = Q_{\text{tot}} - Q_{\text{tl}} = Q_m C_p (T_{\text{inlet}} - T_{\text{outlet}}). \tag{7}$$

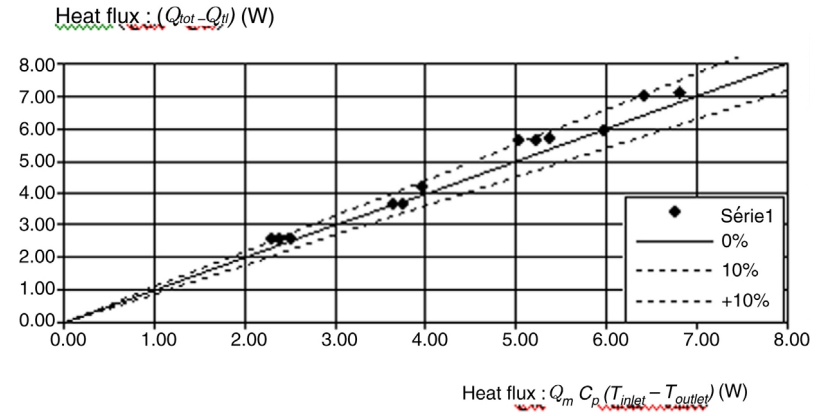

Fig. 5. Heat balance closing for several conditions of flow rate and wall temperature.

From Eq. (7), it can be noticed that the heating flux Q_h can be experimentally determined by two methods, either by measuring the total electric power supplied without thermal losses ($Q_{tot} - Q_{tl}$), or directly by measuring the inlet and outlet temperatures of the liquid ($Q_m C_p (T_{inlet} - T_{outlet})$). Experimentally, the two methods must give the same values and in Fig. 5 the good agreement of the results can be checked.

So as the heat flux calculated with the inlet and outlet temperatures is of good accuracy (about 2% deviation), and as a mean deviation of about 10% between the two methods was observed, the uncertainty of the measurements presented in the following results is 12%.

3.4. Volume vapour fraction measurement

Because of the difficulty of obtaining images of high quality in the structured channel, the vapour–liquid mixture has been filmed at the outlet of the structured part.

The volume vapour fraction has been estimated for each experiment by recording the liquid–vapour flow at the outlet of the structured channel with a numerical and high speed camera with a constant speed of 400 fps for a total duration of 5 s. Then, we used the software Visilog 5.4, which sorts each pixel of the recorded images to decide whether it belongs to the liquid or vapour phase (Fig. 6), depending on the greyscale of the pixel. The surface vapour fraction can then be estimated.

The assumption of equality between the surface vapour fraction and the volume vapour fraction was made considering the values of the Bond number which compares the influence of gravity to the capillarity forces:

$$Bo = \frac{(\rho_{liq} - \rho_{vap}) \cdot g \cdot D_h^2}{\sigma}. \tag{8}$$

In the case of pure water flowing through a channel of 200 μm characteristic dimension, the value of the Bond number is 0.0067 (density of liquid: 1000 kg m^{-3}; density of vapour at atmospheric pressure: 0.58 kg m^{-3}; surface tension of water: 0.0582 N m^{-1} at 98 °C).

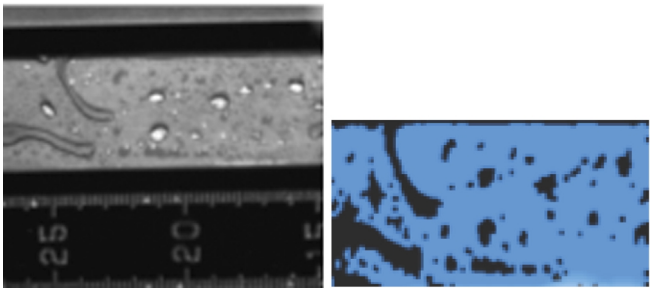

Fig. 6. A typical image for the estimation of the volume vapour fraction, before (left) and after image analysis (right).

As this value is far below 0.6, it can be considered that the vapour bubbles fill all the intersection between two square obstacles in the channel, so we can reasonably assume the volume fraction of the vapour, α, to be equal to the surface volume fraction. As the silicon is completely wetted by the water, a very thin layer of liquid remains between the bubble of vapour and the wall, which is rapidly vaporized and does not perturb the volume vapour fraction measurement.

4. Experimental results

4.1. Results

The tests were conducted for the following ranges of wall temperature and mass flow rate:

- Wall temperature: 120–150 °C.
- Mass flow rate: 0.125–1 ml min^{-1} (Reynolds number: 2.1–9.7).

The boiling heat transfer coefficients are calculated with the equation

$$h = \frac{Q_{\text{vap}}}{\Omega \cdot (T_{\text{w}} - T_{\text{sat}})}. \tag{9}$$

Fig. 7 presents the values of the boiling heat transfer coefficient as a function of the Reynolds number (with $D_{\text{h}} = 200$ μm and with characteristic values of liquid water) for different conditions of wall temperatures.

We can observe that at Reynolds numbers lower than about 7 and for relatively low wall temperatures (below 135 °C), the heat transfer coefficient is almost independent of the Reynolds number ($Nu = 0.5$–0.6), except at 150 °C, where the heat transfer is influenced by the flow rate. Furthermore, for all temperatures, a dramatic decrease of the heat transfer coefficient can be noticed at higher Reynolds values. The decrease of the observed heat transfer coefficient corresponds to the critical heat flux when a gas blanket appears between the wall and the liquid and induces a resistance to the heat transfer. The heat transfer coefficients obtained below the critical heat flux are comparable to those obtained by Peng [4] for pure water (6000 W $\text{m}^{-2}\,\text{°C}^{-1}$ for $Re = 150$) in tubes of steel with a hydraulic diameter

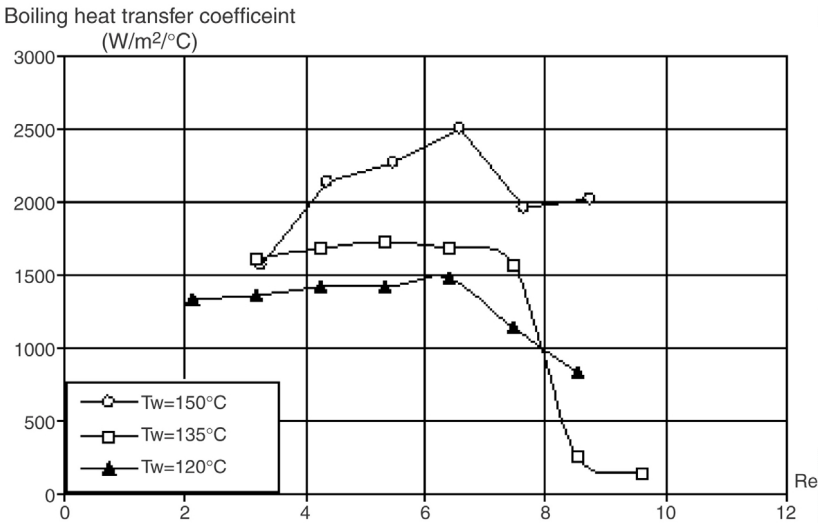

Fig. 7. Heat transfer coefficient versus Reynolds number for different wall temperatures.

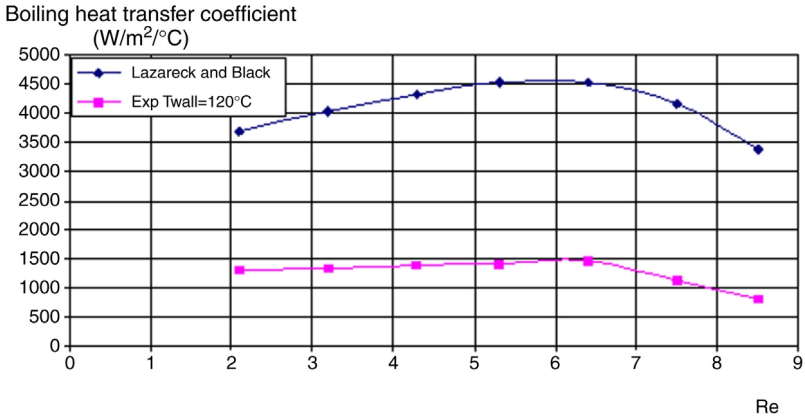

Fig. 8. Comparison of the experimental results to the correlation proposed by Lazareck and Black in 1982.

of 150 μm and a wall temperature of 130 °C. In a recent publication, Qu and Mudawar [5] report heat transfer coefficients between 25 and 45 kW m^{-2} $°C^{-1}$ in channels of 231 μm × 712 μm cross-section. No clear explanation has yet been found to explain such a difference.

4.2. Comparison of the experimental results with the literature

The heat transfer coefficients obtained for $T_w = 120$ °C are compared (Fig. 8) to the values given by the correlation proposed by Lazareck and Black in 1982 [6]:

$$h = \frac{Nu_3}{Nu_4}\left[30\left(Re^{0.857}Boi^{0.714}\frac{k_{\text{liq}}}{D_{\text{h}}}\right)\right] \tag{10}$$

$$Nu_3 = 8.235(1 - 1.883\beta + 3.767\beta^2 - 5.814\beta^3 + 5.361\beta^4 - 2.0\beta^5) \tag{11}$$

$$Nu_4 = 8.235(1 - 2.042\beta + 3.3085\beta^2 - 2.477\beta^3 - 1.058\beta^4 - 0.186\beta^5). \tag{12}$$

This correlation has been obtained for the boiling of a refrigerant (R-133) in straight mini-channels (2.31 mm) made of steel.

The same tendency is observed for the two curves: a slight increase of the heat transfer coefficient below a Reynolds number of 7, and a sudden decrease after this point. However, even if the values of the heat transfer coefficient are of the order of a few thousands, a factor 3 is observed throughout the tested range of Re. This discrepancy may be explained by the difference of geometry and the nature of the materials used in the two structures.

5. Experimental determination of the slip ratio

An alternative way to determine the boiling heat transfer coefficient would be to measure the mass vapour fraction X and to use the following relation, obtained from the heat balance equation:

$$h = \frac{Q_m \cdot X \cdot \Delta H_{\text{vap}}}{\Omega \cdot (T_{\text{w}} - T_{\text{sat}})}. \tag{13}$$

However, the mass vapour fraction X cannot be measured directly; only the volume vapour fraction α can be obtained by non-intrusive visual observation.

As the vapour and liquid phases flow at different velocities, the relation between the mass and volume fraction has to account for the slip ratio factor S:

$$X = \frac{1}{1 + \frac{\rho_{\text{liq}}.(1-\alpha)}{\rho_{\text{vap}}.S.\alpha}}. \tag{14}$$

The slip ratio S can be estimated either from experimental data obtained directly in our boiling flow micro-system or by using correlations, such as the relation proposed by Hewitt [2], but which has not been validated in micro-systems. These correlations were developed in non-boiling conditions (air and water for large tubes) and give unrealistic heat transfer coefficient values. Therefore, instead of determining the boiling heat transfer coefficient, it would be more appropriate to compare the experimental values of S with the correlation values, to check the deviation of such a relation in micro-boiling flow.

5.1. Calculation of the slip ratio from the experiments

Using a combination of Eqs. (6) and (14) it is possible, by measuring the volume vapour fraction α, to estimate the experimental slip ratio with the following relation:

$$S = \frac{X}{1 - X} \cdot \frac{1 - \alpha}{\alpha} \cdot \frac{\rho_{\text{liq}}}{\rho_{\text{vap}}}. \tag{15}$$

Table 1
Experimental slip ratio versus slip ratio calculated via Hewitt correlation for $T_{wall} = 135\,^{\circ}C$

Mass flow rate (g s^{-1})	Volume of vapour fraction	S Experimental	S Hewitt
6.25E–03	0.56	50 000	8 950
8.33E–03	0.35	90 000	18 980
1.00E–02	0.29	110 000	22 990
1.25E–02	0.46	10 000	10 290
1.46E–02	0.45	4 000	10 100

5.2. The predicted slip ratio

The slip ratio can also be estimated via different correlations as proposed by Hewitt [2]:

$$S = 1 + E_1 * \left(\frac{y}{1 + y * E_2} - y * E_2 \right)^{0.5} \tag{16}$$

with the following expressions for the parameters E_1, E_2 and y:

$$E_1 = 1.578 * R_{e,\mathrm{liq}}^{-0.19} * \left(\frac{\rho_{\mathrm{liq}}}{\rho_{\mathrm{vap}}} \right)^{0.22} \tag{17}$$

$$E_2 = 0.0273 * W_{e,\mathrm{liq}} * R_{e,\mathrm{liq}}^{-0.51} * \left(\frac{\rho_{\mathrm{liq}}}{\rho_{\mathrm{vap}}} \right)^{-0.08} \tag{18}$$

$$y = \frac{(1 - \alpha) \cdot S}{\alpha}. \tag{19}$$

The calculation method is iterative and requires one to estimate the value of S—an a priori value of S for calculating the parameters y, E_1 and E_2 to be introduced in Eq. (16) to give a new value of S. If the recalculated value is different from the estimate, a new iteration is performed with another value of S.

5.3. Comparison of experimental and correlative results

The slip ratios S given by the two methods (experimental and correlation) are reported in Table 1, for different values of the volume vapour fraction.

We can observe that the experimental slip ratio is much higher than the one predicted using the correlations of Hewitt, leading us to reject them in their current form as regards use in micro-system flow under boiling conditions. The problem is that this method does not take into account the effect of confinement (very important at the micro-scale) and the boiling conditions. A possibility for getting a better estimate of the slip ratio would be to modify the Hewitt relations by introducing the confinement number and/or the boiling number.

6. Conclusion

The heat transfer performances of the micro-vaporizer have been measured for different conditions, and it appears that, for low wall temperatures (below 135 °C) and low

Reynolds numbers (below 7), the flow rate does not influence the heat transfer. These values of the heat transfer coefficient are comparable to those obtained by Peng, but are much lower than those presented by Qu and Mudawar. This difference has not yet been explained.

For the same values of Re and higher wall temperatures, the heat transfer coefficient is dependent on the flow rate. The sudden decrease of the heat transfer, for Re higher than 7, can be explained by the critical heat flux, which causes a blanket of vapour to form between the wall and the liquid.

Concerning the conversion of the volume vapour into the mass vapour fraction using a slip ratio, the correlations proposed by Hewitt for conventional ducts underpredict the slip ratio for low flow rates, but overpredict it for high flow rates. A possible explanation is that these equations do not take into account the phase change and the reduced dimensions of the system. This led us to reject them for micro-system flow in their current form. Further work on this subject has to be done, either to modify Hewitt's correlations, or to propose new ones which would allow a better prediction of the mass vapour fraction from the volume vapour fraction. One way to modify the correlations proposed by Hewitt would be to introduce some parameters such as the confinement (Co) and boiling (Boi) numbers to take into account those two effects.

Acknowledgements

The research presented in this paper was funded by the European Union (project number: EU ENK6CT200000110).

References

[1] E.R. Delsman, E.V. Rebrov, M.H.J.M. de Croon, J.C. Schouten, G.J. Kramer, V. Cominos, T. Richter, T.T. Veenstra, A. van den Berg, P.D. Cobden, F.A. de Bruijn, C. Ferret, U. d'Ortona, L. Falk, Mirth-e: micro reactor technology for hydrogen technology and electricity, in: Proceedings of IMRET 5, Strasbourg, 2001, pp. 368–374.

[2] G.F. Hewitt, Void fraction, in: G. Hetsroni (Ed.), Handbook of Multiphase Systems, McGraw-Hill, 1982, pp. 76–85 (Chapter 2).

[3] C. Ferret, L. Falk, U. d'Ortona, M.N. Pons, T.T. Veenstra, F. Lim, A. van den Berg, Using image analysis to measure the heat transfer coefficient in a silicon micro-evaporator, in: Proceedings of IMRET 6, New Orleans, 2002.

[4] X.F. Peng, G.P. Peterson, B.X. Wang, Flow boiling of binary mixtures in microchanneled plates, Int. J. Heat Mass Transfer 39 (1996) 1257–1264.

[5] W. Qu, I. Mudawar, Flow boiling heat transfer in two-phase micro-channel heat sinks—I. Experimental investigation and assessment of correlation methods, Int. J. Heat Mass Transfer 46 (2003) 2755–2771.

[6] G.M. Lazareck, S.H. Black, Evaporative heat transfer, pressure drop and critical heat flux in a small vertical tube with R-113, Int. J. Heat Mass Transfer 25 (1982) 945–960.